Struct Multidisc Optim (2005) 29: 257–271
DOI 10.1007/s00158-004-0482-0

RESEARCH PAPER

Z. Dimitrovová

A new methodology to establish upper bounds on open-cell foam homogenized moduli

Received: 23 June 2003 / Revised manuscript received: 30 April 2004 / Published online: 26 October 2004

Abstract The methodology to determine upper bounds on homogenized linear elastic moduli of cellular solids, described for the two-dimensional case in Dimitrovová and Faria (1999), is extended to three-dimensional open-cell foams. Besides the upper bounds the methodology provides necessary and sufficient conditions on the optimal media. These conditions are written in terms of generalized internal forces and geometrical parameters. In some cases dependence on internal forces can be replaced by geometrical expressions. In such cases optimality of some medium under consideration can be verified directly from the microstructure, without any additional calculation. Some of the bounds derived in this paper have not yet been published along with a proof of their optimality.

Keywords Energy methods · Homogenization techniques · Open-cell foams · Optimal microstructure · Optimization · Upper bounds on effective moduli

1 Introduction

Cellular solids can either be found in nature or manufactured by foaming of polymers, metals and ceramics, or by other technologies, such as e.g. chemical vapor deposition (CVD) and direct metal laser sintering (DMLS). They have a wide range of applications, namely in the absorption of the kinetic energy from impacts, or as thermal and electrical insulators. To exploit these properties fully and efficiently, suitable methodologies allowing a detailed characterization of the cellular solid's behavior are needed. In this article we will examine upper bounds on homogenized linear elastic moduli.

A cellular solid (a foam) is composed of an interconnected network of solid beams and shell parts, which can be assigned to cells, that are repeated in the medium. Two essential features characterize cellular media:

Z. Dimitrovová
DEM/ISEL and IDMEC/IST, Instituto Superior Técnico, Av. Rovisco pais, 1, 1049-001 Lisbon, Portugal
E-mail: zdimitro@dem.ist.utl.pt

- The size of voids is very small compared to the size of the full medium, and thus homogenization techniques (see Duvaut (1976), Bensoussan et al. (1978), Suquet (1985), Bakhvalov and Panasenko (1989), Nemat-Nasser and Hori (1993)) can be used in the determination of the effective properties.
- The relative density is low, usually below 0.3 (Gibson and Ashby 1988). As a consequence at least one dimension of the solid phase (thickness) at the cell level is small compared to the characteristic cell size. This condition justifies the use of structural theories in homogenization calculations instead of the full 3D elasticity model.

Cellular solids may be classified as closed-cell, partly open-cell and open-cell foams. In this work we will restrict our analysis only to open-cell foams, which consist solely of solid beams. The name repetitive lattice structures can then also be adopted.

Several works have dealt with effective elastic properties of open-cell foams or repetitive lattice structures, however, upper bounds on them are rarely analyzed. The main monograph on cellular solids was published by Gibson and Ashby (1988). Extensive work by Christensen has been dedicated to the characterization of effectively isotropic open-cell microstructures, where the response is governed by bending or direct (axial) resistance, (Christensen 1994, 1995). In Christensen (1995) the values of the upper bound on the effective bulk and shear moduli are presented. The value of the bulk modulus bound was also addressed by several other works, but only in the sense of an effective property of some particular microstructure, see e.g. Warren and Kraynik (1988, 1997), Kraynik and Warren (1994), Zhu et al. (1997).

Methodologies for effective properties determination can be discrete or continuous. Discrete approaches are usually based on micromechanics. They exploit either the periodicity or the regularity of the medium under consideration. In the former case calculations are performed on a unit or a basic cell, while in the latter case either a representative volume element or a typical joint is used. For instance in Kraynik and Warren (1994) and Warren and Kraynik (1997) effective moduli are determined by considering a tetrahedral joint (Kelvin foam) under an assumption of affine displacements. Application of this methodology to a medium with randomly placed basic cells of the regular cubic lattice also yields the maximum shear response. In this context, the work of Dimitrovová (1999) could also be mentioned, where a detailed discussion of the applicability of the orientational averaging to periodic cells is given. Among other works, (Grenestedt 1999; Li et al. 2003) should also be mentioned. Continuum modeling of repetitive lattice structures is reviewed by Noor (1988). The literature review in this paragraph is far from being complete because it is not the aim of this paper to determine homogenized moduli, but their upper bounds.

The inverse problem of identifying microstructures that achieve prescribed effective properties has also been extensively studied (see, e.g. Sigmund (1994), Neves et al. (2000), Gibianski and Sigmund (2000), Guedes et al. (2003)). These methods exploit homogenization techniques, starting with a basic cell whose shape must be specified in advance, and the available material is then optimally distributed within it.

Cellular solids can be viewed as two-phase composites with void and solid (generally nonhomogeneous) phases. Determination of bounds on composite effective properties has been the subject of considerable research for many years. One may argue that there is no need for any new methodology, since the bounds for foams can be obtained from the composite two-phase ones, just by the introduction of zero void properties. This is true in 2D, but in 3D the optimal foams must contain shell parts in some regimes of optimality (Allaire and Kohn 1993), therefore upper bounds on homogenized moduli of open-cell foams are strictly lower than those for general foams and the development of a new methodology addressing this issue is fully justified.

Only upper bounds on effective elastic moduli will be examined, because lower bounds for media with one void phase are zero. Without loss of generality only open-cell foams with periodic microstructure will be considered, because in a medium with random microstructure, a representative volume element can be chosen so that a medium created by its periodic repetition will have the same effective properties as the original random one. The contribution of this paper is the extension of the methodology proposed by Dimitrovová and Faria (1999) from 2D to 3D. The methodology is based on homogenization theory and does not require any restriction on the basic cell shape or arrangement. The influence of the boundary layer is not accounted for and it is assumed that the basic cell contains a finite number of structural members, i.e. beams or bars. Upper bounds are derived by a bounding procedure using results from linear algebra and the Voigt bound basic assumption (Hill 1963). The main advantage of the new methodology is that from the bounding procedure the necessary and sufficient conditions characterizing the optimal media will immediately follow. These conditions are written in terms of generalized internal forces and geometrical parameters. The proposed methodology recovers the well-known bounds for effectively isotropic open-cell foams, although with a different proof. The main contribution lies in the identification of new bounds on effective shear moduli of open-cell microstructures with effective cubic symmetry. In such cases dependence on internal forces in maximality conditions can be replaced by geometrical expressions, implying that the optimality of the medium under consideration can be verified directly from the microstructure, without any additional calculation. Approximations inherent to the methodology are commonly used structural simplifications. Limitations are based on the assumption of a finite number of structural members in the basic cell, allowing only the identification of single-scale microstructures, which implicitly excludes multiple-rank laminates (see e.g. Allaire and Aubry (1999)) and the Hashin's spheres assemblage (Hashin 1962).

The paper is organized as follows. The methodology is reviewed in Sect. 2, namely in Sect. 2.1 simplified assumptions and basic relations are introduced, in Sect. 2.2 it is shown that the optimal media can be initially sought within a specific class of micro-trusses (the term will be explained later on) and in Sect. 2.3 the methodology is reviewed within this restricted class. Bounds are proven in Sect. 3 along with optimal media microstructures specification. The paper is concluded in Sect. 4 with the discussion and analysis of the developments achieved.

2 Review of the new methodology

2.1 Simplifying assumptions and basic relations

The basic cell, ϑ, defined as the (smallest) region of a periodic medium that can compose the full medium by periodic repetition, will be conveniently rescaled to V, where the spatial microvariable $\mathbf{y}$ is introduced. It is assumed that V contains a finite number of beams and that the solid phase is homogeneous and isotropic. Therefore the term material volume fraction can be used instead of relative density.

There are two extreme possibilities for the structural model of a joint between the beams composing the foam: (i) pin joint and (ii) rigid joint. A pin joint cannot transmit bending moments and therefore allows rotations of the structural members connected to it. Consequently non-loaded structural member with two pin joints can only support internal forces acting in the direction of the line connecting the joints. On the other hand a rigid joint preserves the angles between the beams connected to it. If all joints are rigid, the term *micro-frame medium* can be used; on the other hand *not necessarily straight* structural members connected by pin joints will be named *micro-truss media*. Therefore any micro-frame medium has its related micro-truss, which is obtained by switching the behavior of rigid joints to pin joints. In reality joint behavior is somewhere between these two extreme cases and should be represented by a flexible joint. Pin-joint behavior can be achieved either by a special construction allowing for rotations of the connected members or as a limit case: if the beams connected to a given joint have uniform cross-sectional areas and the material volume fraction tends to zero, then the flexible joint approaches pin-joint behavior.

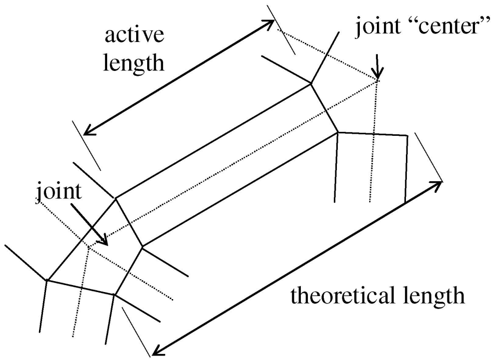

Fig. 1 Introduction of theoretical and active lengths

In structural theories beams are defined by their middle axes and joints can be replaced by single points (joint "centers") located in the middle axes intersection. The term theoretical length will be used to identify the middle axis length between joint centers and active length to identify the same length shortened by the parts inside the joints (Fig. 1). Small discrepancies when middle axes do not intersect exactly at a single point will not be considered.

We will address only open-cell foams with effective isotropy or cubic symmetry. The tensor of effective elastic constants can thus be written in dimensionless matrix form as:

$$\mathbf{C}^* = \begin{pmatrix} \mathbf{C}_1^* & \mathbf{0} \\ \mathbf{0} & \mathbf{C}_2^* \end{pmatrix}, \tag{1}$$

where $\mathbf{C}_2^* = G_2^* \mathbf{I}$ and

$$\mathbf{C}_1^* = \begin{pmatrix} K^* + 4G_1^*/4 & K^* - 2G_1^*/4 & K^* - 2G_1^*/4 \\ & K^* + 4G_1^*/4 & K^* - 2G_1^*/4 \\ symm. & & K^* + 4G_1^*/4 \end{pmatrix}. \tag{2}$$

Here $\mathbf{I}$ stands for the unit 3 by 3 matrix and $\mathbf{0}$ for the zero 3 by 3 matrix. Effective engineering constants K, G_1 and G_2 are the homogenized bulk and two shear moduli, respectively. Their *dimensionless values with respect to the solid phase Young's modulus* E_s are identified as: $K^* = K/E_s$, $G_1^* = G_1/E_s$ and $G_2^* = G_2/E_s$. A medium is effectively isotropic when $G_1^* = G_2^* = G^*$. The above matrix form of the fourth-order tensor of elastic constants (see Lekhnitskii (1981)) in terms of the engineering constants K^*, G_1^* and G_2^* is presented in Hashin and Shtrikman (1962).

At first, the aim is to determine each of the macroscopic engineering constants in terms of the generalized internal forces, which will form the initial relation for the bounding procedure. The global strain energy density W can be expressed for isotropic media as:

$$W = \frac{1}{2E_s}\left(\frac{\Sigma_M^2}{K^*} + \frac{\mathbf{\Sigma}_D : \mathbf{\Sigma}_D}{2G^*}\right) \tag{3}$$

and for media with effective cubic symmetry as:

$$W = \frac{1}{2E_s}\left\{\frac{\Sigma_M^2}{K^*} + \frac{\Sigma_{D,12}^2 + \Sigma_{D,31}^2 + \Sigma_{D,23}^2}{G_2^*}\right.$$
$$\left. + \frac{\tilde{\Sigma}_{D,12}^2 + \tilde{\Sigma}_{D,31}^2 + \tilde{\Sigma}_{D,23}^2}{6G_1^*}\right\}, \tag{4}$$

where Σ_M and $\mathbf{\Sigma}_D$ are the volumetric and deviatoric parts of the global stress tensor $\mathbf{\Sigma}$, $\mathbf{\Sigma}_D : \mathbf{\Sigma}_D = \Sigma_{D,ij}\Sigma_{D,ij}$ (summation convention is adopted) and $\tilde{\Sigma}_{D,12} = \Sigma_{D,11} - \Sigma_{D,22}$, $\tilde{\Sigma}_{D,31} = \Sigma_{D,33} - \Sigma_{D,11}$, $\tilde{\Sigma}_{D,23} = \Sigma_{D,22} - \Sigma_{D,33}$. The test macroloads, to be applied on the medium and consequently on the basic cell, can be chosen so that only one effective engineering constant will be left in (3) or (4), and can be thus expressed independently of the others and in terms of $\mathbf{\Sigma}$ components and W. Examples of these macroloads are specified in Table 1. It is seen that the corresponding macrostrain $\mathbf{E}$ must fulfill similar conditions. The macrostrain $\mathbf{E}$ is connected to the macrostress $\mathbf{\Sigma}$ by $\mathbf{\Sigma} = E_s\mathbf{C}^* \cdot \mathbf{E}$, where
$\mathbf{\Sigma} = \{\Sigma_{11}, \Sigma_{22}, \Sigma_{33}, \Sigma_{23}, \Sigma_{31}, \Sigma_{12}\}^T$,
$\mathbf{E} = \{E_{11}, E_{22}, E_{33}, 2E_{23}, 2E_{31}, 2E_{12}\}^T$ and "$\cdot$" stands for matrix multiplication.

$\mathbf{\Sigma}$ and W can be expressed with the help of an averaging operator applied on the local characteristics, σ and w, (Suquet 1985):

Table 1 Test macroloads and the corresponding specification of the macrostress and the macrostrain

Macroload	Property	Specification of $\mathbf{\Sigma}$	Specification of $\mathbf{E}$
$\mathbf{\Sigma}^K$	K^*	$\Sigma = \Sigma_{11} = \Sigma_{22} = \Sigma_{33} \neq 0$, $\Sigma_{ij} = 0\ \forall i \neq j$	$E = E_{11} = E_{22} = E_{33} \neq 0$, $E_{ij} = 0\ \forall i \neq j,\ 3K^* = \Sigma/(E\ E_s)$
$\mathbf{\Sigma}^{1G}$	G_1^*	$\Sigma_{11} + \Sigma_{22} + \Sigma_{33} = 0,\ \exists k;\ \Sigma_{kk} \neq 0$, $\Sigma_{ij} = 0\ \forall i \neq j$	$E_{11} + E_{22} + E_{33} = 0,\ E_{ij} = 0\ \forall i \neq j$, $2G_1^* = \Sigma_{kk}/(E_{kk}\ E_s)\ \forall k^\dagger$
$\mathbf{\Sigma}^{2G}$	G_2^*	$\Sigma_{11} = \Sigma_{22} = \Sigma_{33} = 0,\ \exists i \neq j;\ \Sigma_{ij} \neq 0$	$E_{11} = E_{22} = E_{33} = 0$, $2G_2^* = \Sigma_{ij}/\left(E_{ij}\ E_s\right)\ \forall i \neq j^\dagger$
$\mathbf{\Sigma}^G$	G^*	$\Sigma_{11} + \Sigma_{22} + \Sigma_{33} = 0,\ \exists k;\ \Sigma_{kk} \neq 0$, $\exists i \neq j;\ \Sigma_{ij} \neq 0$	$E_{11} + E_{22} + E_{33} = 0$, $2G^* = \Sigma_{ij}/\left(E_{ij}\ E_s\right)\ \forall i, j^\dagger$

(†if the macrostress component is different from zero)

$$\Sigma_{jk} = \frac{1}{|V|}\int_{V^\sharp} \sigma_{jk}\,\mathrm{d}\mathbf{y} = \frac{1}{|V|}\sum_i \int_{V_i^\sharp} \sigma_{jk}^i\,\mathrm{d}\mathbf{y} = \sum_i \left\langle \sigma_{jk}^i \right\rangle, \tag{5}$$

$$W = \frac{1}{|V|}\int_{V^\sharp} w\ \mathrm{d}\mathbf{y} = \frac{1}{|V|}\sum_i \int_{V_i^\sharp} w^i\,\mathrm{d}\mathbf{y} = \sum_i \left\langle w^i \right\rangle, \tag{6}$$

where σ^i and w^i are the local stress and the local strain energy density corresponding to the i^{th} beam (i-beam). The volume of the full cell is $|V|$ while the volume of the i-beam is$|V_i^\sharp|$. $|V_i^\sharp|$ is composed of the volume corresponding to the active length plus the corresponding volume in the connected parts within the joints, so that $|V_i^\sharp \bigcap V_j^\sharp| = 0\ \forall i \neq j$ and $\sum_i |V_i^\sharp| = |V^\sharp|$. $V^\sharp$ is the volume of the material part in the cell. Due to the periodic repetition it is not necessary to treat separately the case when the i-beam is cut by the boundary of the cell.

Next, it is necessary to express contributions of each i-beam, $\langle\sigma^i\rangle$ and $\langle w^i\rangle$, in terms of generalized internal forces. Looking at $\langle\sigma^i\rangle$, the formula from Nemat-Nasser and Hori (1993)

$$\left\langle \sigma_{mj}^i \right\rangle = \frac{1}{\left|V_i^\sharp\right|}\int_{\partial V_i^\sharp} \sigma_{jk}^i n_k b_m\,\mathrm{d}\mathbf{S} = \frac{1}{\left|V_i^\sharp\right|}\int_{\partial V_i^\sharp} t_j^i b_m\,\mathrm{d}\mathbf{S} \tag{7}$$

can be exploited. In (7) **b** is the position vector of the points on $\partial V_i^\sharp$ and **t** is the boundary traction. If **t** is self-equilibrated, then $\left\langle\sigma^i\right\rangle$ is symmetric and the integral in (7) does not depend on the origin of the coordinate system for **b**. Expression for $\left\langle w^i\right\rangle$ can be, as usual, simplified by considering that generalized internal forces act over theoretical lengths and that the contribution from the joints is negligible.

2.2 Micro-trusses with straight bars of constant cross-sectional area versus micro-frames

Optimal low-density micro-frame open-cell foams will be defined as those for which the related micro-truss is optimal. Justification of this definition and more details on optimal micro-trusses are presented in this subsection, namely it will be proven that optimal micro-trusses can only be composed from straight bars with constant cross section.

In order to justify the definition stated above it is necessary to verify that a curved beam cannot make part of the optimal low-density media. Let us suppose that the i-beam of a micro-frame basic cell is curved. Then a local coordinate system (z_1, z_2) can be introduced so that z_1 connects the joint centers (Fig. 2). The middle axis of the beam is given by $z_2 = a(z_1)$ and r designates the curved coordinate. Let us separate the beam of active length from the joints by the cuts shown in Fig. 2. It is assumed that there exists a plane containing the i-beam middle curve and that the macroload acts in a way that the generalized internal forces in the beam cuts are also contained in this plane. The geometrical parameters $\alpha(r)$, α_{0k}, α_{0m}, h_k, h_m, v_k, v_m, l, p, the generalized internal forces in the beam cuts F, B and D and other local auxiliary coordinate systems $(\tilde{z}_1, \tilde{z}_2)$ and $(\hat{z}_1, \hat{z}_2)$

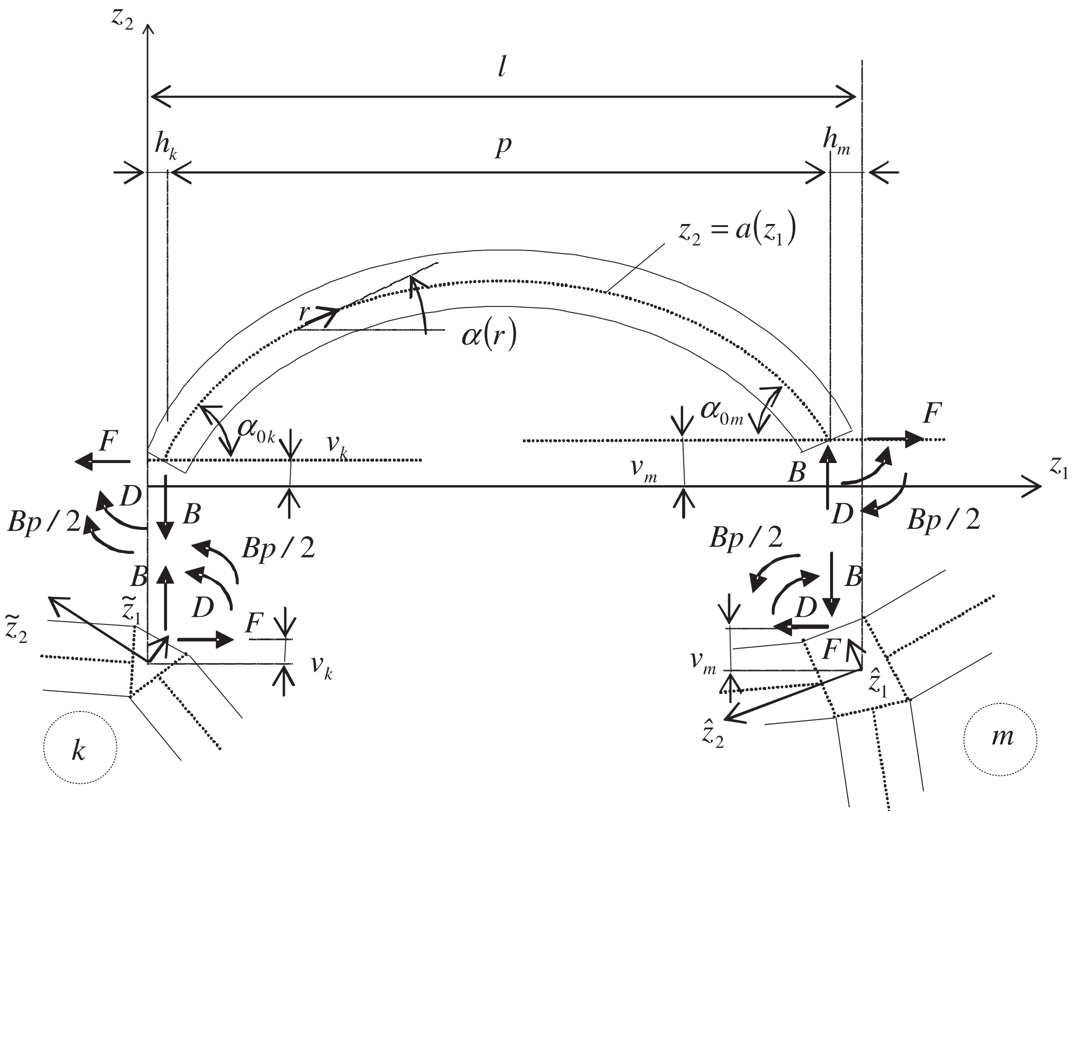

Fig. 2 Specification of the curved i-beam

are specified in Fig. 2. l and p are projections of the theoretical and the active lengths on z_1 and the bending moment along the beam is separated into its (average) constant (D) and "antisymmetric" parts.

For the i-beam let us express the average quantities $\langle \sigma^i \rangle$ and $\langle w_i \rangle$ in terms of the generalized internal forces and discuss the possibility of its position in an optimal medium. The superscript "i" will be omitted for the sake of simplicity, where possible without confusion. It must be pointed out that local stress averaging cannot be performed over the theoretical length, because it would cause joint overlapping. Thus the i-beam average stress $\langle \sigma \rangle$ must be expressed as $\langle \sigma \rangle = \langle \sigma_{bm} \rangle + \langle \sigma_{jk} \rangle + \langle \sigma_{jm} \rangle$, where the contribution with subscript "*bm*" relates to the beam with active length and those with "*jk*" and "*jm*" subscripts relate to the left (k) and right (m) adjacent joints parts, respectively. Strict application of (7), in the previous expression, would imply integration over the internal faces of the joints, which is complicated. To overcome these difficulties one can define $\langle \tilde{\sigma} \rangle = \langle \sigma_{bm} \rangle + \langle \tilde{\sigma}_{jk} \rangle + \langle \tilde{\sigma}_{jm} \rangle$, where $\langle \tilde{\sigma}_{jk} \rangle$ and $\langle \tilde{\sigma}_{jm} \rangle$ stand only for the contribution of the faces where the beam was cut. Then $\langle \tilde{\sigma}_{jk} \rangle$ and $\langle \tilde{\sigma}_{jm} \rangle$ are coordinate system dependent and therefore their coordinate systems must be uniquely defined in a way applicable to any beam from the basic cell. Coordinate systems $(\tilde{z}_1, \tilde{z}_2)$ and $(\hat{z}_1, \hat{z}_2)$ are introduced as specified in Fig. 2. With respect to (z_1, z_2), (7) yields:

(see Equation (8) on this page)

With respect to $(\tilde{z}_1, \tilde{z}_2)$ and $(\hat{z}_1, \hat{z}_2)$ one can obtain:

$$|V| \left\langle \tilde{\sigma}'_{jk} \right\rangle = \begin{pmatrix} Fh_k + Bv_k & -Fv_k + Bh_k \\ -Bp/2 - D & 0 \end{pmatrix} \text{ and}$$

$$|V| \left\langle \tilde{\sigma}'_{jm} \right\rangle = \begin{pmatrix} Fh_m - Bv_m & Fv_m + Bh_m \\ -Bp/2 + D & 0 \end{pmatrix} \tag{9}$$

which after rotation to (z_1, z_2) yields:

$$|V| \left\langle \tilde{\sigma}'_{jk} \right\rangle = \begin{pmatrix} \begin{array}{c} Fh_k \\ +\frac{1}{2} Bp \sin\alpha_{0k} \cos\alpha_{0k} \\ +D \sin\alpha_{0k} \cos\alpha_{0k} \end{array} & \begin{array}{c} Bh_k \\ +\frac{1}{2} Bp \sin^2\alpha_{0k} \\ +D \sin^2\alpha_{0k} \end{array} \\ \\ \begin{array}{c} Fv_k \\ -\frac{1}{2} Bp \cos^2\alpha_{0k} \\ -D \cos^2\alpha_{0k} \end{array} & \begin{array}{c} Bv_k \\ -\frac{1}{2} Bp \sin\alpha_{0k} \cos\alpha_{0k} \\ -D \sin\alpha_{0k} \cos\alpha_{0k} \end{array} \end{pmatrix} \tag{10}$$

and

$$|V| \left\langle \tilde{\sigma}'_{jm} \right\rangle = \begin{pmatrix} \begin{array}{c} Fh_m \\ -\frac{1}{2} Bp \sin\alpha_{0m} \cos\alpha_{0m} \\ +D \sin\alpha_{0m} \cos\alpha_{0m} \end{array} & \begin{array}{c} Bh_m \\ +\frac{1}{2} Bp \sin^2\alpha_{0m} \\ -D \sin^2\alpha_{0m} \end{array} \\ \\ \begin{array}{c} -Fv_m \\ -\frac{1}{2} Bp \cos^2\alpha_{0m} \\ +D \cos^2\alpha_{0k} \end{array} & \begin{array}{c} -Bv_m \\ +\frac{1}{2} Bp \sin\alpha_{0m} \cos\alpha_{0m} \\ -D \sin\alpha_{0m} \cos\alpha_{0m} \end{array} \end{pmatrix}, \tag{11}$$

which finally gives

$$\langle \tilde{\sigma} \rangle = \frac{l}{|V|} \begin{pmatrix} F & B \\ 0 & 0 \end{pmatrix}. \tag{12}$$

Origins of the coordinate systems (z_1, z_2) and $(\tilde{z}_1, \tilde{z}_2)$ are coincident, therefore only the face of joint (m) and the face of beam corresponding to it could be considered to obtain (12). It is necessary to point out that the reason for non-symmetry of $\langle \tilde{\sigma} \rangle$ is the omission of the contributions from the internal faces of the joints in (9)–(11), as explained above. This does not mean any inaccuracy, because after rotation of all beam contributions to the cell coordinate system and summation over all the beams, the final expression for $\mathbf{\Sigma}$ will be complete and symmetric.

When a general curved beam under a general macroload is considered, local coordinate system (z_1, z_2) connecting the joint centers can also be introduced. Then it is necessary to replace internal force B by B_1 and B_2, bending moment D by D_1 and D_2 and to introduce torsion moment T. Following the same procedure as above, one obtains:

$$\langle \tilde{\sigma} \rangle = \frac{l}{|V|} \begin{pmatrix} F & B_1 & B_2 \\ 0 & 0 & 0 \\ 0 & 0 & 0 \end{pmatrix}. \tag{13}$$

It is important to realize that (13) has the same form as it would have for a related straight beam with theoretical length l, arbitrary cross-sectional area variation and with the same generalized internal forces in cuts. Therefore there is no distinction between the $\langle \sigma \rangle$ contribution of a straight or a curved beam to $\mathbf{\Sigma}$. Moreover (13) does neither include the constant part of bending moments D_1 and D_2 nor the torsion moment T. If the i-beam had pin joints, then from equilibrium $B_1 = B_2 = 0$. We recall that, in order to express $\mathbf{\Sigma}$, (13) should be rotated to the basic cell coordinates and summed over all the beams.

$$|V| \langle \sigma_{bm} \rangle = \begin{pmatrix} \begin{array}{c} Fp - \frac{1}{2} Bp \left(\sin\alpha_{0k} \cos\alpha_{0k} - \sin\alpha_{0m} \cos\alpha_{0m} \right) \\ -D \left(\sin\alpha_{0k} \cos\alpha_{0k} + \sin\alpha_{0m} \cos\alpha_{0m} \right) \end{array} & \begin{array}{c} \frac{1}{2} Bp \left(\cos^2\alpha_{0k} + \cos^2\alpha_{0m} \right) \\ +D \left(\cos^2\alpha_{0k} - \cos^2\alpha_{0m} \right) \end{array} \\ \\ \begin{array}{c} -F \left(v_k - v_m \right) + \frac{1}{2} Bp \left(\cos^2\alpha_{0k} + \cos^2\alpha_{0m} \right) \\ +D \left(\cos^2\alpha_{0k} - \cos^2\alpha_{0m} \right) \end{array} & \begin{array}{c} \frac{1}{2} Bp \left(\sin\alpha_{0k} \cos\alpha_{0k} - \sin\alpha_{0m} \cos\alpha_{0m} \right) \\ +B \left(v_k - v_m \right) + D \left(\sin\alpha_{0k} \cos\alpha_{0k} + \sin\alpha_{0m} \cos\alpha_{0m} \right) \end{array} \end{pmatrix}. \tag{8}$$

Now the average $\langle w\rangle$ will be determined. For the sake of simplicity it is again firstly assumed that a curved beam and the generalized forces are contained in a plane. As usual strain energy density corresponding to shear forces can be omitted. Then one can write:

$$\langle w\rangle = \frac{1}{2\,|V|\,E_s}\left(\int\limits_{(a)}\frac{N^2(r)}{A(r)}\,\mathrm{d}r + \int\limits_{(a)}\frac{M^2(r)}{I(r)}\,\mathrm{d}r\right), \tag{14}$$

where $A(r)$ and $I(r)$ stand for cross-sectional area and moment of inertia, respectively, $N(r)$ and $M(r)$ are normal forces and bending moments and (a) stands for the integration along the curved theoretical length of the beam. It might be remarked that using theoretical lengths and overlapping in joints is an allowable and common simplification in strain energy expression. In accordance with this approximation, the originally introduced generalized forces F, B and D in beam cuts do not have to change.

A cross-sectional area A_0 of a related straight beam with constant cross section and the same volume as the original curved one, can be introduced by (overlapping in junctions can also be neglected here):

$$A_0 l = \int\limits_0^l A(z_1)\sqrt{1+(a'(z_1))^2}\,\mathrm{d}z_1\,, \tag{15}$$

where $a'(z_1) = \frac{\mathrm{d}a(z_1)}{\mathrm{d}z_1}$.

Because there is no distinction between the $\langle\sigma\rangle$ contribution of straight or curved beams to $\mathbf{\Sigma}$, let us minimize $\langle w\rangle$ in order to discuss the position of the i-beam in an optimal medium. This minimization must be performed over all possible shapes $a(z_1)$ and volume distributions along the middle curve:

$$\begin{aligned}
&2E_s\,|V| \min_{a(z_1);A(r);I(r)} \langle w\rangle \\
&= \min_{a(z_1);A(r);I(r)}\left(\int\limits_{(a)}\frac{N^2(r)}{A(r)}\,\mathrm{d}r + \int\limits_{(a)}\frac{M^2(r)}{I(r)}\,\mathrm{d}r\right) \\
&\geq \min_{a(z_1);A(r)}\int\limits_{(a)}\frac{N^2(r)}{A(r)}\,\mathrm{d}r + \min_{a(z_1);I(r)}\int\limits_{(a)}\frac{M^2(r)}{I(r)}\,\mathrm{d}r\,.
\end{aligned} \tag{16}$$

Equality in (16) can be achieved if the minimizing shape and volume distribution are the same for both terms in the last part of (16).

The normal force distribution can be written as:

$$N(r) = F\cos\alpha(r) + B\sin\alpha(r)\,. \tag{17}$$

Therefore:

$$\int\limits_{(a)}\frac{N^2(r)}{A(r)}\,\mathrm{d}r = \int\limits_0^l \frac{\left(F+Ba'(z_1)\right)^2}{A(z_1)\sqrt{1+(a'(z_1))^2}}\,\mathrm{d}z_1\,. \tag{18}$$

Using the Schwarz inequality in the form:
(see Equation (19) on next page)
gives the following inequality:

$$\int\limits_0^l \frac{\left(F+Ba'(z_1)\right)^2}{A(z_1)\sqrt{1+(a'(z_1))^2}}\,\mathrm{d}z_1 \geq F^2\frac{l}{A_0}\,. \tag{20}$$

Equality in (20) or (19) can only be achieved if $\frac{F+Ba'(z_1)}{A(z_1)\sqrt{1+(a'(z_1))^2}}$ is constant with respect to z_1, which implies that the beam must be straight and with constant cross-sectional area. Then the normal force contribution to $\langle w\rangle$ does not include B.

The bending moment distribution can be expressed as:

$$M(z_1) = D + Fa(z_1) + B\left(\frac{l}{2} - z_1\right). \tag{21}$$

When minimizing conditions for the contribution of normal forces to $\langle w\rangle$ are used, it is sufficient to look at $\int\limits_0^l \left(D + B\left(\frac{l}{2}-z_1\right)\right)^2 \mathrm{d}z_1 = D^2 l + B^2 l^3/12$. The optimal media requires $D = 0$ because D does not appear in (12). If moreover $B = 0$, as a consequence of constant cross-sectional area and material volume fraction going to zero, then the contribution from the bending moment is zero and the last term in (16) reaches its trivial minimum. Extension of this statement to a general curved beam under general macroload is clear; there would only be one more integral in form of (21) and a separate T contribution, which can be required to be zero, because T does not appear in (13).

This justifies the definition of optimal media stated at the beginning of this subsection and proves that optimal micro-trusses must be composed of straight bars with constant cross-sectional areas. Nevertheless the bending contribution is not excluded from the optimal media when it has micro-frame behaviour.

In summary, optimal open-cell foams can be sought within the class of micro-trusses with straight bars of constant cross section. In this class the bound can be expressed as a linear function of the material volume fraction, s, as shown in Dimitrovová and Faria (1999) and as clarified in Sect. 3. Related optimal micro-frames can develop non-zero bending moments, but only in their antisymmetric form (in terms of B_1 and/or B_2). If bending moments are presented, the corresponding effective engineering constant, written as a Taylor's expansion in s, contains a quadratic term (a detailed discussion is provided in Dimitrovová and Faria (1999)). The tangent at $s = 0$, i.e. the linearized bound, relates to the same property of the corresponding micro-truss. Please note however (see Fig. 3) that for a particularly high material volume fraction, s_0, there can exist a micro-frame with a higher elastic property than that obtained from the optimal micro-truss. These cases are of no interest here since *for low-density media only the initial slope (linearized property) matters*. For the same reasons media with only bending response are strictly excluded from the class of optimal micro-frames because the corresponding micro-truss is a kinematical mechanism and the linearized bound is zero.

$$F^2 l^2 = \left(\int_0^l \left(F + Ba'(z_1) \right) \mathrm{d}z_1 \right)^2 = \left(\int_0^l \frac{F + Ba'(z_1)}{\sqrt{A(z_1)} \sqrt[4]{1 + (a'(z_1))^2}} \left(\sqrt{A(z_1)} \sqrt[4]{1 + (a'(z_1))^2} \right) \mathrm{d}z_1 \right)^2$$

$$\leq \left(\int_0^l \frac{\left(F + Ba'(z_1) \right)^2}{A(z_1) \sqrt{1 + (a'(z_1))^2}} \mathrm{d}z_1 \right) \left(\int_0^l A(z_1) \sqrt{1 + (a'(z_1))^2} \mathrm{d}z_1 \right) = A_0 l \int_0^l \frac{\left(F + Ba'(z_1) \right)^2}{A(z_1) \sqrt{1 + (a'(z_1))^2}} \mathrm{d}z_1 \qquad (19)$$

It was shown in Dimitrovová and Faria (1999) that if bulk modulus is under consideration, then the components of macrostress necessary to express this property do not contain a B contribution. So, bending moments are excluded from optimal media, not only in the limit at $s = 0$, but in the full range of low-density s values. This result is readily extendable to 3D.

In Sect. 3.2, optimal micro-trusses for the shear modulus G_1^* of media with effective cubic symmetry will be fully geometrically specified. In this case it will be seen that switching to micro-frames will not develop bending moments. So the upper bound is also linear here within the validity of structural theories. The bending contribution is present only in the isotropic shear G^* and in G_2^*.

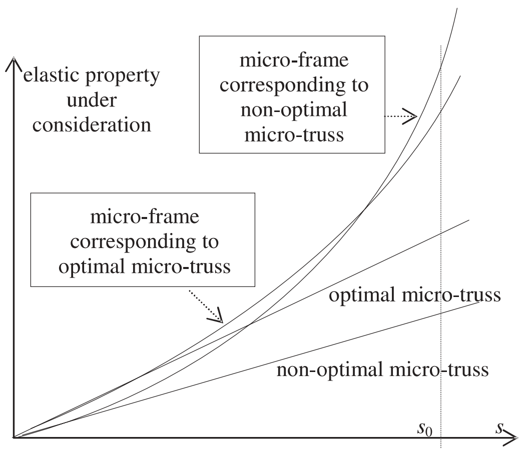

Fig. 3 Specification of optimal media response

2.3 Review of the methodology in the class of micro-truss media with straight bars of constant cross section

In the class of micro-trusses, normal force is the only generalized internal force in the medium. Let an arbitrary basic cell consisting of n bars be assumed. The contributions $\left\langle \sigma^i \right\rangle$ and $\langle w_i \rangle$ of each i-bar with theoretical length l_i, cross-sectional area A_i and normal force N_i can be specified in the following way (compare with (13)):

$$\left\langle \sigma^i \right\rangle = \frac{N_i l_i}{|V|} \begin{pmatrix} \cos^2\varphi_i \sin^2\theta_i & \sin\varphi_i \cos\varphi_i \sin^2\theta_i & \cos\varphi_i \sin\theta_i \cos\theta_i \\ & \sin^2\varphi_i \sin^2\theta_i & \sin\varphi_i \sin\theta_i \cos\theta_i \\ symm. & & \cos^2\theta_i \end{pmatrix}, \qquad (22)$$

where the two spherical angles $\theta_i \in \langle 0, \pi)$ and $\varphi_i \in \langle 0, 2\pi)$ specify the i-bar position with respect to the cell coordinates y_j, $j = 1, 2, 3$, (Fig. 4); and (see (16) and (20))

$$\langle w_i \rangle = \frac{1}{2|V|E_s} \left(N_i^2 \frac{l_i}{A_i} \right). \qquad (23)$$

Let the following notation be introduced:

$$\Omega_{1,i} = \cos^2\varphi_i \sin^2\theta_i, \ \Omega_{2,i} = \sin^2\varphi_i \sin^2\theta_i,$$

$$\Omega_{3,i} = \cos^2\theta_i;$$

$$\Phi_{1,i} = \sin\varphi_i \sin\theta_i \cos\theta_i, \ \Phi_{2,i} = \cos\varphi_i \sin\theta_i \cos\theta_i,$$

$$\Phi_{3,i} = \sin\varphi_i \cos\varphi_i \sin^2\theta_i;$$

$$\Psi_{1,i} = \sin^2\varphi_i \sin^2\theta_i - \cos^2\theta_i,$$

$$\Psi_{2,i} = \cos^2\theta_i - \cos^2\varphi_i \sin^2\theta_i,$$

$$\Psi_{3,i} = \cos(2\varphi_i) \sin^2\theta_i; \qquad (24)$$

then the vectors $\mathbf{N}$, $\mathbf{R}$, $\mathbf{Q}$ and $\mathbf{L}$ (compare with Dimitrovová and Faria (1999)) can be defined as:

$$\mathbf{N} = \left\{ N_1 \sqrt{\frac{l_1}{A_1}}, N_2 \sqrt{\frac{l_2}{A_2}}, \ldots, N_n \sqrt{\frac{l_n}{A_n}} \right\};$$

$$\mathbf{R}_j = \left\{ \Omega_{j,1}\sqrt{l_1 A_1}, \Omega_{j,2}\sqrt{l_2 A_2}, \ldots, \Omega_{j,n}\sqrt{l_n A_n} \right\},$$

$j = 1, 2, 3$;

$$\mathbf{Q}_j = \left\{ \Phi_{j,1}\sqrt{l_1 A_1}, \Phi_{j,2}\sqrt{l_2 A_2}, \ldots, \Phi_{j,n}\sqrt{l_n A_n} \right\},$$

$j = 1, 2, 3$;

$$\mathbf{L} = \left\{ \sqrt{l_1 A_1}, \sqrt{l_2 A_2}, \ldots, \sqrt{l_n A_n} \right\}. \qquad (25)$$

In addition, let us denote:

$$\mathbf{P}_1 = \mathbf{R}_2 - \mathbf{R}_3, \ \mathbf{P}_2 = \mathbf{R}_3 - \mathbf{R}_1, \ \mathbf{P}_3 = \mathbf{R}_1 - \mathbf{R}_2. \qquad (26)$$

Thus:

$$\mathbf{P}_j = \left\{ \Psi_{j,1}\sqrt{l_1 A_1}, \Psi_{j,2}\sqrt{l_2 A_2}, \ldots, \Psi_{j,n}\sqrt{l_n A_n} \right\},$$

$j = 1, 2, 3 \qquad (27)$

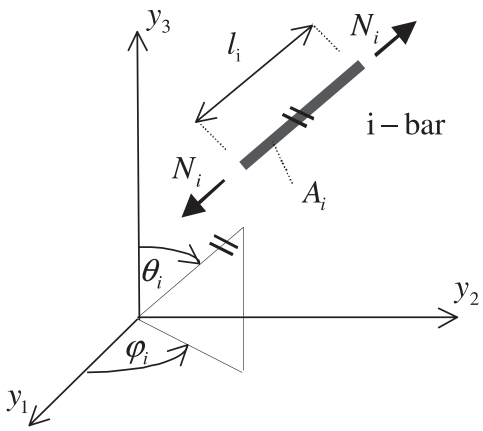

Fig. 4 Specification of the i-bar within the basic cell

and it holds:

$$\mathbf{P}_1+\mathbf{P}_2+\mathbf{P}_3=\mathbf{0},\ \mathbf{R}_1+\mathbf{R}_2+\mathbf{R}_3=\mathbf{L}\,,$$
$$\|\mathbf{P}_1\|^2+\|\mathbf{P}_2\|^2+\|\mathbf{P}_3\|^2+$$
$$\|\mathbf{Q}_1\|^2+\|\mathbf{Q}_2\|^2+\|\mathbf{Q}_3\|^2=2\,\|\mathbf{L}\|^2\ , \tag{28}$$

where $\|\ \|$ is the Euclidean norm. The material volume fraction, s, can be approximated neglecting higher-order terms as:

$$s=\frac{\|\mathbf{L}\|^2}{|V|}. \tag{29}$$

Taking into account (24)–(25), (22) can be substituted into (5) giving:

$$\boldsymbol{\Sigma}=\frac{1}{|V|}\mathbf{S}\cdot\mathbf{N}^T$$
$$=\frac{1}{|V|}\{\mathbf{R}_1,\mathbf{R}_2,\mathbf{R}_3,\mathbf{Q}_1,\mathbf{Q}_2,\mathbf{Q}_3\}^T\cdot\mathbf{N}^T \tag{30}$$

and (23) into (6) as:

$$W=\frac{\|\mathbf{N}\|^2}{2\,|V|\,E_s}\,, \tag{31}$$

where $\mathbf{S}$ will be called a modified static matrix.

As written in Sect. 2.1, a particular engineering constant can be expressed, from (3) or (4), independently of the others, if the corresponding macroload from Table 1 is applied. Then expressions (30)–(31) can be introduced and the initial expression for the bounding procedure, in terms of normal forces and geometrical parameters, is obtained. The bounding procedure is performed using basic knowledge from linear algebra and the Voigt assumption for the upper bound derivation (uniform local strain), and the bound is finally expressed as a linear function of the material volume fraction. *Maximality conditions* on possible normal forces are then obtained as conditions that ensure equality with the bound. The specifications in Table 1 provide the *additional constraints* on the possible normal forces that can be developed in an optimal medium. Using the maximality conditions, these additional constraints can be written in terms of microstructure geometrical parameters, as will be seen in Sect. 3.

For more details on the Voigt assumption and bound see e.g. Hill (1963). We only remark that, when local strains are uniform throughout the medium, then they are equal to the macroscopic strain and the global engineering constant corresponding to such a macroload reaches its maximum. Since micro-truss media are characterized by the bar middle axes, which (except for the joints) correspond to the "direction" of the local strain, the Voigt assumption implies that the local displacements of the bar middle axes, $\mathbf{u}$, coincide with the linear part of displacements, i.e. $u_i=E_{ij}y_j$ (summation convention is adopted). This requirement states *necessary maximality conditions* on possible normal forces, which can be written as:

$$\mathbf{S}^T\cdot\mathbf{E}=\mathbf{N}^T/E_s\,. \tag{32}$$

Maximality conditions (32) are not sufficient because the requirement of uniform strain does not exclude bars with zero normal force (*zero bars*). More facts about relation between optimal micro-frames and the Voigt bound are given in the Appendix.

Obviously, upper bounds determined in the way described in this subsection could be extremely large and unrealistic because no restrictions such as topological connectivity or joint equilibrium were considered. However, if a physical medium saturating the bound can be found, the bound would be proven to be optimal. This is actually achieved in all the cases considered in this paper.

3 Linearized bounds on effective moduli

3.1 Bulk modulus K^* (for effective isotropy or cubic symmetry)

If the macroload $\boldsymbol{\Sigma}^K$ (Table 1) is imposed, then starting with (3), introducing (30)–(31), (28) and (29), the bulk modulus K^* can be expressed as:

$$K^*=\frac{\Sigma_M^2}{2E_sW}=\frac{|V|}{\|\mathbf{N}\|^2}\left(\frac{(\mathbf{R}_1+\mathbf{R}_2+\mathbf{R}_3)\cdot\mathbf{N}^T}{3\,|V|}\right)^2$$
$$=\frac{1}{9\,|V|}\frac{\left(\mathbf{L}\cdot\mathbf{N}^T\right)^2}{\|\mathbf{N}\|^2}\le\frac{s}{9}\,, \tag{33}$$

providing the maximality condition

$$\mathbf{N}\parallel\mathbf{L}\,, \tag{34}$$

(i.e. local stresses are required to be constant all over the bars) and the bound $K_+^*=s/9$. Using (34), additional constraints from Table 1 can be written in terms of geometrical parameters as:

$$\mathbf{R}_1\cdot\mathbf{L}^T=\mathbf{R}_2\cdot\mathbf{L}^T=\mathbf{R}_3\cdot\mathbf{L}^T\ \&\ \mathbf{Q}_j\perp\mathbf{L}\ \forall j=1,2,3\,. \tag{35}$$

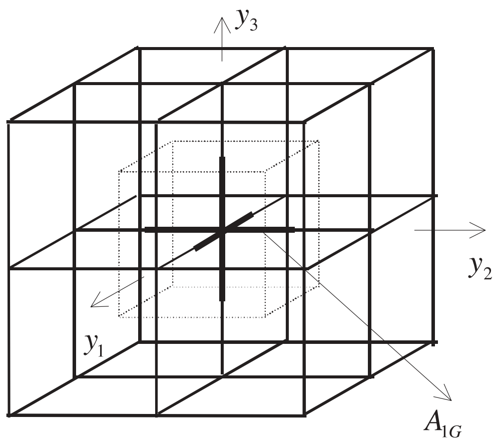

Fig. 5 The regular cubic lattice

Equation (32), which should also be implemented, does not bring, in this case, anything new. It is seen that it corresponds directly to (34), after conditions from Table 1 had been implemented, $\mathbf{N} = \frac{\Sigma}{3K^*\mathbf{L}}$. One can check that in this case (32) ensures not only the necessary but also sufficient maximality condition, because zero bars are excluded as $N_i \sim A_i \neq 0\ \forall i$, where "$\sim$" means proportionality.

The conditions stated in (34)–(35) are the necessary and sufficient conditions on K^*-optimal media. Equation (34) cannot be expressed only in terms of geometrical parameters and therefore verification of K^*-optimality of some medium requires the determination of the normal forces in $\mathbf{N}$. The bound is optimal because several known media saturate it. The simplest K^*-optimal medium is the regular cubic lattice (Fig. 5) (see Warren and Kraynik (1988), Dimitrovová (1999)), where it is easy to verify conditions (34)–(35). The class of periodic K^*-optimal media can be extended by the class of media with random microstructure, where a basic cell of some K^*-optimal medium appears in the representative volume element with all possible rotations with the same probability. Because the bulk modulus is invariant under orientational averaging, the bulk modulus of the new random medium will be the same as for the corresponding periodic medium (Dimitrovová 1999).

3.2 Shear modulus G_1^* (for effective cubic symmetry)

If macroload $\mathbf{\Sigma}^{1G}$ (see Table 1) is imposed, then one has:

$$G_1^* = \frac{1}{6|V|}\frac{\left(\mathbf{P}_1\cdot\mathbf{N}^T\right)^2+\left(\mathbf{P}_2\cdot\mathbf{N}^T\right)^2+\left(\mathbf{P}_3\cdot\mathbf{N}^T\right)^2}{\|\mathbf{N}\|^2}$$
$$= \frac{s}{6}\,\frac{\sum\limits_{j=1,2,3}\left\|\mathbf{P}_j\right\|^2\cos^2\left(\mathbf{N},\mathbf{P}_j\right)}{\|\mathbf{L}\|^2}$$
$$= \frac{s}{3}\,\frac{\sum\limits_{j=1,2,3}\left\|\mathbf{P}_j\right\|^2\cos^2\left(\mathbf{N},\mathbf{P}_j\right)}{\sum\limits_{j=1,2,3}\left\|\mathbf{P}_j\right\|^2+\sum\limits_{j=1,2,3}\left\|\mathbf{Q}_j\right\|^2}\,. \tag{36}$$

According to Table 1, additional constraints on possible $\mathbf{N}$ are:

$$\mathbf{N}\perp\mathbf{L}\ \&\ \mathbf{N}\perp\mathbf{Q}_j \quad \forall j=1,2,3\,. \tag{37}$$

If $\mathbf{Q}_j = \mathbf{0}\ \forall j=1,2,3$ and $\mathbf{N} \parallel \mathbf{P}_j\ \forall j=1,2,3$, then the maximum in (36) would be $s/3$. However no physical medium could fulfill all these conditions, as will be shown in the following. In order to determine the real maximum, it is necessary to realize that any $\mathbf{\Sigma}^{1G}$ can be written as a linear combination of three basic cases $\Sigma_{22} = -\Sigma_{33} = 1$, $\Sigma_{33} = -\Sigma_{11} = 1$ and $\Sigma_{11} = -\Sigma_{22} = 1$. In each of these local strains must be uniform according to (32) and the value of the corresponding G_1^* must be the same, as specified in Table 2.

Using superposition, the necessary maximality condition from Table 2 reads:

$$\mathbf{N} = \frac{1}{2G_1^*}\left(\mu_1\mathbf{P}_1+\mu_2\mathbf{P}_2+\mu_3\mathbf{P}_3\right)$$
$$= \lambda_1\mathbf{P}_1+\lambda_2\mathbf{P}_2+\lambda_3\mathbf{P}_3\,, \tag{38}$$

where the coefficients μ_j express the particular basic cases combination corresponding to the imposed macroload. Additional constraints from Table 2 must be satisfied simultaneously, giving:

$$\mathbf{Q}_j\perp\mathbf{P}_k \quad \forall j,k=1,2,3\,,$$
$$\|\mathbf{R}_1\| = \|\mathbf{R}_2\| = \|\mathbf{R}_3\|\,,$$
$$\cos\left(\mathbf{R}_1,\mathbf{R}_2\right) = \cos\left(\mathbf{R}_2,\mathbf{R}_3\right) = \cos\left(\mathbf{R}_3,\mathbf{R}_1\right) \tag{39}$$

and

$$\|\mathbf{P}_1\| = \|\mathbf{P}_2\| = \|\mathbf{P}_3\| = 2\sqrt{G_1^*\,|V|}\,. \tag{40}$$

Equation (40) could be obtained directly as the condition ensuring the same G_1^* in all basic cases. If (40) was derived first, then using some statements about finite dimensional spaces, condition (38) is the maximality condition for the sum: $\cos^2(\mathbf{N},\mathbf{P}_1)+\cos^2(\mathbf{N},\mathbf{P}_2)+\cos^2(\mathbf{N},\mathbf{P}_3)$. Here it holds that:

$$\cos^2(\mathbf{N},\mathbf{P}_1)+\cos^2(\mathbf{N},\mathbf{P}_2)+\cos^2(\mathbf{N},\mathbf{P}_3) = 3/2\,. \tag{41}$$

Then the bound $G_{1,+}^* = s/6$ can be obtained from (36) if $\mathbf{Q}_j = \mathbf{0}\ \forall j=1,2,3$. Thus the proof of $G_{1,+}^* = s/6$ would be completed if at least one optimal medium can be found, i.e. if there exists a medium in which $\mathbf{Q}_j = \mathbf{0}\ \forall j=1,2,3$, expressions (38)–(40) hold and no zero bars are contained in it.

In order to justify an existence of such a medium, first of all the spherical angles that will ensure $\mathbf{Q}_j = \mathbf{0}\ \forall j=1,2,3$ must be found. This requirement is equivalent to the condition that

$$\max\left(\left|\Psi_{1,i}\right|+\left|\Psi_{2,i}\right|+\left|\Psi_{3,i}\right|\right) \tag{42}$$

Table 2 Basic load cases in $\mathbf{\Sigma}^{1G}$

Basic case	1.	2.	3.
Macrostress	$\Sigma_{22}=-\Sigma_{33}=1$	$\Sigma_{33}=-\Sigma_{11}=1$	$\Sigma_{11}=-\Sigma_{22}=1$
Macrostrain	$E_{22}=-E_{33}=1/\left(2G_1^*E_s\right)$	$E_{33}=-E_{11}=1/\left(2G_1^*E_s\right)$	$E_{11}=-E_{22}=1/\left(2G_1^*E_s\right)$
Maximality condition from (32)	$\mathbf{N}=\frac{1}{2G_1^*}\mathbf{P}_1$	$\mathbf{N}=\frac{1}{2G_1^*}\mathbf{P}_2$	$\mathbf{N}=\frac{1}{2G_1^*}\mathbf{P}_3$
Additional constraints	$\Vert\mathbf{R}_2\Vert=\Vert\mathbf{R}_3\Vert$, $\mathbf{R}_1\perp\mathbf{P}_1$, $\mathbf{P}_1\perp\mathbf{Q}_j\ \forall j=1,2,3$	$\Vert\mathbf{R}_3\Vert=\Vert\mathbf{R}_1\Vert$, $\mathbf{R}_2\perp\mathbf{P}_2$, $\mathbf{P}_2\perp\mathbf{Q}_j\ \forall j=1,2,3$	$\Vert\mathbf{R}_1\Vert=\Vert\mathbf{R}_2\Vert$, $\mathbf{R}_3\perp\mathbf{P}_3$, $\mathbf{P}_3\perp\mathbf{Q}_j\ \forall j=1,2,3$

Table 3 Characterization of G_1^*-optimal media

Group	1.	2.	3.
Spherical angles	$\varphi_1=0$, $\theta_1=\pi/2$	$\varphi_2=\pi/2$, $\theta_2=\pi/2$	$\theta_3=0$
Values of Ψ_1, Ψ_2, Ψ_3	$0,-1,1$	$1,0,-1$	$-1,1,0$
Values of Ω_1, Ω_2, Ω_3	$1,0,0$	$0,1,0$	$0,0,1$

is obtained for each i. Solution of problem (42) results in three groups of angles, which predict bar directions in an optimal medium, as stated in Table 3. It is therefore convenient to choose a rectangular basic cell with faces perpendicular to the bar directions. Due to the equilibrium in joints only continuous bars passing through the cell can be present. From Table 3 it follows immediately that $\mathbf{R}_1\perp\mathbf{R}_2\perp\mathbf{R}_3$, but in order to ensure $\Vert\mathbf{R}_1\Vert=\Vert\mathbf{R}_2\Vert=\Vert\mathbf{R}_3\Vert$, the following condition must be satisfied:

$$\sum_{1.\ group} l_iA_i=\sum_{2.\ group} l_jA_j=\sum_{3.\ group} l_kA_k\,, \tag{43}$$

i.e. in each of the three perpendicular directions in the cell, the volume of the bars must be the same. It remains to ensure (38) and impose conditions to eliminate zero bars. Let us take for example one continuous bar from the first group. From (38) follows that, all over the bar, $N_i/A_i=\lambda_3-\lambda_2$ holds. Therefore normal forces between the respective joints must be proportional to the cross-sectional areas with the same coefficient of proportionality in each group. Due to the equilibrium in joints, normal forces must be the same within each continuous bar, which implies that the cross-sectional areas are constant within the continuous bar as well.

Let us now summarize the results. $G_{1,+}^*=s/6$ and all G_1^*-optimal media can be *fully geometrically specified* in the following way:
G_1^*-optimal media are continuous lattices for which:

- a rectangular basic cell (with dimensions L_i in y_i-directions, $i=1,2,3$) consisting only of continuous orthogonal bars in the y_i-directions can be found,
- each bar has constant cross-sectional area within the basic cell and the condition $L_1\sum_{i=1}^{n_1}A_i=L_2\sum_{j=1}^{n_1}A_j=L_3\sum_{k=1}^{n_1}A_k$ is satisfied (n_i is the number of bars in the y_i-direction, $i=1,2,3$).

The group of media specified above is the only group of G_1^*-optimal media. They are in fact the 3D extension of the uniform perpendicular lattices (UPL) introduced in Dimitrovová and Faria (1999). The simplest example from this group is the regular cubic lattice (Fig. 5). The value of its G_1^* (not the proof of maximality) could be obtained directly from the G_1^* of its 2D analogue: the regular square lattice. If we denote by s_{2D} and s_{3D} the material volume fractions of 2D and 3D regular lattices, respectively, $s_{2D}=2s_{3D}/3$ holds, and consequently

$$G_1^*=\frac{1}{4}s_{2D}=\frac{1}{6}s_{3D}\,. \tag{44}$$

3.3 Shear modulus G_2^* (for effective cubic symmetry)

First of all, we point out that in 3D there does not exist a rotation of global coordinates that interchanges the positions of G_1^* and G_2^* in $\mathbf{C}^*$, as exists in 2D (see Dimitrovová and Faria (1999)). Thus G_2^*-optimal media cannot be derived from G_1^*-optimal media. For macroload $\mathbf{\Sigma}^{2G}$ one can obtain:

$$G_2^*=\frac{1}{6\,|V|}\frac{\left(\mathbf{Q}_1\cdot\mathbf{N}^T\right)^2+\left(\mathbf{Q}_2\cdot\mathbf{N}^T\right)^2+\left(\mathbf{Q}_3\cdot\mathbf{N}^T\right)^2}{\Vert\mathbf{N}\Vert^2}$$
$$=\frac{s}{3}\,\frac{\sum_{j=1,2,3}\Vert\mathbf{Q}_j\Vert^2\cos^2\left(\mathbf{N},\mathbf{Q}_j\right)}{\sum_{j=1,2,3}\Vert\mathbf{P}_j\Vert^2+\sum_{j=1,2,3}\Vert\mathbf{Q}_j\Vert^2}\,. \tag{45}$$

Additional constraints on possible $\mathbf{N}$ are:

$$\mathbf{N}\perp\mathbf{R}_j\quad\forall j=1,2,3\,. \tag{46}$$

The obvious maximum $s/3$ cannot be achieved by any medium, like in Sect. 3.2. Also combination of 2D results (contrary to (44)) would lead to a wrong conclusion, as can be demonstrated: let only $\Sigma_{23}\neq0$ in $\mathbf{\Sigma}^{2G}$, then an optimal medium should have bars in the directions of the unit square diagonals in the (2,3) planes, according to Dimitrovová and Faria (1999). Analogously, the other load cases $\Sigma_{12}\neq0$ and $\Sigma_{13}\neq0$ imply bar directions in the (1,2) and (1,3) planes, respectively. The 2D result $G_{2,+}^*=s_{2D}/4$ and the fact that $s_{2D}=s_{3D}/3$ thus yield $G_2^*=s_{3D}/12$, because the bar directions stated previously do not coincide. However, it will be proven that $G_{2,+}^*=s/9$.

Table 4 Basic load cases in $\mathbf{\Sigma}^{2G}$

Basic case	1.	2.	3.
Macrostress	$\Sigma_{23}=1$	$\Sigma_{13}=1$	$\Sigma_{12}=1$
Macrostrain	$E_{23}=1/\left(2G_2^*E_s\right)$	$E_{13}=1/\left(2G_2^*E_s\right)$	$E_{12}=1/\left(2G_2^*E_s\right)$
Maximality condition from (32)	$\mathbf{N}=\frac{1}{G_2^*}\mathbf{Q}_1$	$\mathbf{N}=\frac{1}{G_2^*}\mathbf{Q}_2$	$\mathbf{N}=\frac{1}{G_2^*}\mathbf{Q}_3$
Additional constraints	$\mathbf{Q}_1\perp\mathbf{Q}_2\&\mathbf{Q}_1\perp\mathbf{Q}_3$, $\mathbf{Q}_1\perp\mathbf{R}_j\ \forall j=1,2,3$, $\|\mathbf{Q}_1\|^2=G_2^*\,|V|$	$\mathbf{Q}_2\perp\mathbf{Q}_1\&\mathbf{Q}_2\perp\mathbf{Q}_3$, $\mathbf{Q}_2\perp\mathbf{R}_j\ \forall j=1,2,3$, $\|\mathbf{Q}_2\|^2=G_2^*\,|V|$	$\mathbf{Q}_3\perp\mathbf{Q}_1\&\mathbf{Q}_3\perp\mathbf{Q}_2$, $\mathbf{Q}_3\perp\mathbf{R}_j\ \forall j=1,2,3$, $\|\mathbf{Q}_3\|^2=G_2^*\,|V|$

Table 5 Characterization of G_2^*-optimal media

Group	1.	2.	3.	4.
Spherical angles	$\cos\varphi_1=\frac{1}{\sqrt{2}}$, $\sin\varphi_1=\frac{1}{\sqrt{2}}$, $\cos\theta_1=\frac{1}{\sqrt{3}}$, $\sin\theta_1=\frac{\sqrt{2}}{\sqrt{3}}$	$\cos\varphi_2=\frac{1}{\sqrt{2}}$, $\sin\varphi_2=\frac{1}{\sqrt{2}}$, $\cos\theta_2=-\frac{1}{\sqrt{3}}$, $\sin\theta_2=\frac{\sqrt{2}}{\sqrt{3}}$	$\cos\varphi_3=-\frac{1}{\sqrt{2}}$, $\sin\varphi_3=\frac{1}{\sqrt{2}}$, $\cos\theta_3=\frac{1}{\sqrt{3}}$, $\sin\theta_3=\frac{\sqrt{2}}{\sqrt{3}}$	$\cos\varphi_4=-\frac{1}{\sqrt{2}}$, $\sin\varphi_4=\frac{1}{\sqrt{2}}$, $\cos\theta_4=-\frac{1}{\sqrt{3}}$, $\sin\theta_4=\frac{\sqrt{2}}{\sqrt{3}}$
Values of Φ_1, Φ_2, Φ_3	$1/3, 1/3, 1/3$	$-1/3, -1/3, 1/3$	$1/3, -1/3, -1/3$	$-1/3, 1/3, -1/3$
Values of Ω_1, Ω_2, Ω_3	$1/3, 1/3, 1/3$	$1/3, 1/3, 1/3$	$1/3, 1/3, 1/3$	$1/3, 1/3, 1/3$

An arbitrary $\mathbf{\Sigma}^{2G}$ can be expressed as a linear combination of three basic cases (Table 4). Using superposition, the necessary maximality condition reads:

$$\begin{aligned}\mathbf{N} &= \frac{1}{G_2^*}\left(\mu_1\mathbf{Q}_1+\mu_2\mathbf{Q}_2+\mu_3\mathbf{Q}_3\right)\\ &= \lambda_1\mathbf{Q}_1+\lambda_2\mathbf{Q}_2+\lambda_3\mathbf{Q}_3\,,\end{aligned} \tag{47}$$

where the coefficients μ_i express the specific combination of basic cases corresponding to the imposed macroload. Additional constraints are:

$$\mathbf{Q}_j\perp\mathbf{R}_k \quad \forall j,k=1,2,3\ \&\ \mathbf{Q}_1\perp\mathbf{Q}_2\perp\mathbf{Q}_3 \tag{48}$$

and

$$\|\mathbf{Q}_1\|=\|\mathbf{Q}_2\|=\|\mathbf{Q}_3\|=\sqrt{G_2^*\,|V|}\,. \tag{49}$$

If (49) were derived first, then using some statements about finite dimensional spaces, (47) is the maximality condition for the sum of cosines from (45), like in Sect. 3.2. Now, due to the orthogonality of $\mathbf{Q}_j$, the sum of cosines is equal to 1, therefore $G_{2,+}^*=s/9$ if at least one optimal medium exists, i.e. if there can be found a medium in which $\mathbf{P}_j=\mathbf{0}\ \forall j=1,2,3$, (47)–(49) hold and no zero bars are contained. The requirement $\mathbf{P}_j=\mathbf{0}\ \forall j=1,2,3$ is equivalent to the condition that

$$\max\left(\left|\Phi_{1,i}\right|+\left|\Phi_{2,i}\right|+\left|\Phi_{3,i}\right|\right) \tag{50}$$

is obtained for each i. Solutions of (50) yield four groups of angles, as specified in Table 5, corresponding to the unit cube main diagonals. It is not convenient to choose a basic cell with eight faces (perpendicular to the bar directions), because the regular octahedron does not fill space. It is better to assume a rectangular cell according to Fig. 6. The conditions $\mathbf{Q}_j\perp\mathbf{R}_k\ \forall j,k=1,2,3$ imply, again, the same bar volume constraint within each group:

$$\begin{aligned}&\sum_{1.\ group} l_iA_i=\sum_{2.\ group} l_jA_j\\ &=\sum_{3.\ group} l_kA_k=\sum_{4.\ group} l_rA_r\,,\end{aligned} \tag{51}$$

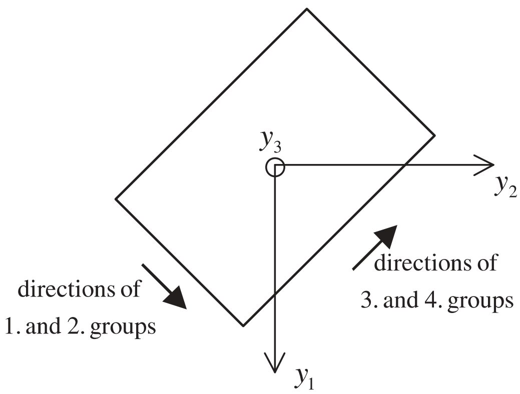

Fig. 6 Rectangular cell for G_2^*-optimal media, top view

which, in a sequel, guarantees mutual perpendicularity of $\mathbf{Q}_j$, $j = 1, 2, 3$, while (49) is satisfied directly.

It remains to ensure that (47) holds and impose conditions to eliminate zero bars. Let us take one bar from the first group. From (47) it directly follows that, in each part between joints of this bar, $N_i/A_i = (-\lambda_1 + \lambda_2 - \lambda_3)/3$ holds. Thus normal forces must be proportional to cross-sectional areas with the same coefficient of proportionality in each group, in other words, in bars of each group local stresses must be the same: $\sigma_1, \sigma_2, \sigma_3, \sigma_4$, respectively. Because four possible directions of bars exist, it cannot be directly concluded that due to the equilibrium in joints only continuous bars are included in the cell. However, this statement can be justified in the following way. Obviously

$$\sigma_1 = (-\lambda_1 + \lambda_2 - \lambda_3)/3\,,\ \sigma_2 = (\lambda_1 - \lambda_2 - \lambda_3)/3\,,$$
$$\sigma_3 = (-\lambda_1 - \lambda_2 + \lambda_3)/3\,,\ \sigma_4 = (\lambda_1 + \lambda_2 + \lambda_3)/3 \qquad (52)$$

hold. Let us take a joint and suppose that a member from each group is presented there as continuous. Contributions to the cell coordinate directions are given in Table 6. Consequently, equilibrium in the joint reads:

$$\sigma_1\left(A_{1,m} - A_{1,m-1}\right) + \sigma_2\left(A_{2,n} - A_{2,n-1}\right) -$$
$$\sigma_3\left(A_{3,r} - A_{3,r-1}\right) - \sigma_4\left(A_{4,s} - A_{4,s-1}\right) = 0\,,$$

$$\sigma_1\left(A_{1,m} - A_{1,m-1}\right) + \sigma_2\left(A_{2,n} - A_{2,n-1}\right) +$$
$$\sigma_3\left(A_{3,r} - A_{3,r-1}\right) + \sigma_4\left(A_{4,s} - A_{4,s-1}\right) = 0\,,$$

$$\sigma_1\left(A_{1,m} - A_{1,m-1}\right) - \sigma_2\left(A_{2,n} - A_{2,n-1}\right) +$$
$$\sigma_3\left(A_{3,r} - A_{3,r-1}\right) - \sigma_4\left(A_{4,s} - A_{4,s-1}\right) = 0\,, \qquad (53)$$

where the first subscript to cross-sectional areas denotes the group and the second expresses order number within the group. Equation (53) must be satisfied for any σ_i, $i = 1, 2, 3, 4$, consequently the cross-sectional areas must be either the same (resulting in a continuous bar with constant cross-sectional area) or zero (the group is not contained in the joint), which completes the justification.

In summary, $G^*_{2,+} = s/9$ and all G^*_2-optimal media can be *fully geometrically specified* in the following way:
G^*_2-optimal media are continuous lattices for which:

- a rectangular basic cell, according to Fig. 6, where only continuous bars in four directions specified by Table 5 are present, can be found,
- each continuous bar has constant cross-sectional area and (51) holds.

Table 6 Contributions of the local stresses to the coordinate directions

	σ_1	σ_2	σ_3	σ_4
y_1	$1/\sqrt{3}$	$1/\sqrt{3}$	$-1/\sqrt{3}$	$-1/\sqrt{3}$
y_2	$1/\sqrt{3}$	$1/\sqrt{3}$	$1/\sqrt{3}$	$1/\sqrt{3}$
y_3	$1/\sqrt{3}$	$-1/\sqrt{3}$	$1/\sqrt{3}$	$-1/\sqrt{3}$

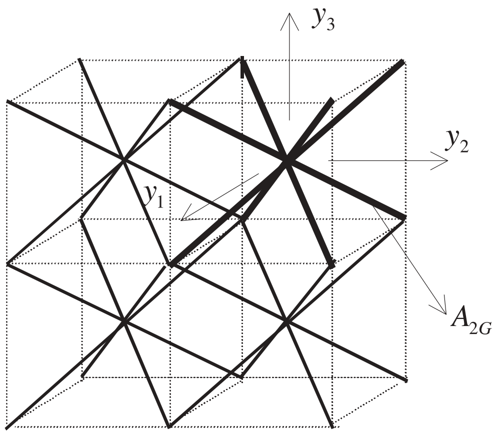

Fig. 7 The regular cube-diagonal lattice

The group of media described above is the only group of G^*_2-optimal media. The name for such media was introduced in Dimitrovová and Faria (1999) as uniform diagonal lattices (UDL). The simplest example from this group is the regular cube-diagonal lattice in Fig. 7.

3.4 Shear modulus G^* (for effective isotropy)

In this case conclusions from the two previous sections can be exploited. Let us assume that we already have a G^*-optimal medium. Macroloads $\mathbf{\Sigma}^{1G}$ and $\mathbf{\Sigma}^{2G}$ can be imposed separately on it and the same bounding procedure as in Sects. 3.2–3.3 can be performed. It is only necessary to prevent a geometrical specification that would contradict the possibility of effective isotropy of the medium. Thus:

$$G^* \le \frac{s}{4}\frac{\|\mathbf{P}\|^2}{\|\mathbf{L}\|^2} \text{ and } G^* \le \frac{s}{6}\frac{\|\mathbf{Q}\|^2}{\|\mathbf{L}\|^2}\,, \qquad (54)$$

where subscripts in $\mathbf{P}$ and $\mathbf{Q}$ are omitted for the sake of simplicity. Since the maximum in both relations of (54) must be the same, $\|\mathbf{P}\|^2 = 2\|\mathbf{Q}\|^2/3$ and, taking into account the, last expression of (28), $G^* \le s/15$ can finally be obtained. Therefore $G^*_+ = s/15$, if at least one optimal medium exists. The necessary maximality and additional constraints could be expressed analogously as in Sects. 3.2–3.3 as:

$$\mathbf{N} = \sum_{j=1,2,3} \lambda_j \mathbf{P}_j + \sum_{k=1,2,3} \mu_k \mathbf{Q}_k \qquad (55)$$

and

$$\|\mathbf{R}_1\| = \|\mathbf{R}_2\| = \|\mathbf{R}_3\|\,;\ \|\mathbf{Q}_1\| = \|\mathbf{Q}_2\| = \|\mathbf{Q}_3\|\,;$$
$$\cos(\mathbf{R}_1, \mathbf{R}_2) = \cos(\mathbf{R}_2, \mathbf{R}_3) = \cos(\mathbf{R}_3, \mathbf{R}_1)\,;$$
$$\mathbf{Q}_j \perp \mathbf{R}_k \quad \forall j, k = 1, 2, 3\,;\ \mathbf{Q}_1 \perp \mathbf{Q}_2 \perp \mathbf{Q}_3\,. \qquad (56)$$

Unfortunately, the full geometrical characterization of G^*-optimal media is not possible. Existence of at least one optimal medium can be proven by superposition of the results, namely by combination of the cells of the simplest G^*_1-

and G_2^*-optimal media, see Dimitrovová and Faria (1999) for the conditions under which such a superposition can be done. Let us denote the material volume fractions of the simplest G_1^*- and G_2^*-optimal media as s_{1G} and s_{2G}, respectively. It can be written:

$$G^* = \frac{s_{1G}}{6} = \frac{s_{2G}}{9}\,, \tag{57}$$

yielding $s_{1G} = 2s_{2G}/3$ and consequently ($s = s_{1G} + s_{2G}$ because the bars of the original media do not coincide) $G^* = s/15$ for the combined medium. As a consequence, the relation between cross-sectional areas can be derived as $A_{1G} = 8\sqrt{3}A_{2G}/9$, where, A_{1G} and A_{2G} stand for the cross sections of the original G_1^*- and G_2^*-optimal media, respectively (Figs. 5 and 7). It can be verified that, in this case as well, the bending effect can be superposed directly, as in the 2D analog, as shown in Dimitrovová and Faria (1999).

4 Concluding remarks

It was proven that G_1^*- and G_2^*-optimal media can be geometrically fully specified; they are UPL and UDL, respectively. For neither K^*- nor G^*-optimal media can full geometrical specification of their microstructure be given. It is easy to verify that G_1^*- and K^*-optimal media, assumed either as micro-trusses or as micro-frames, respond only axially, while in G_2^*- and G^*-optimal micro-frames, bending response is always present. The bending contribution is different for different G_2^*- and G^*-optimal media, therefore the nonlinear part is rather difficult to define. However, it can be stated that for low-density media this nonlinear part is not important. Bending contribution can be increased by putting more material close to the joints because the bending moment distribution is antisymmetric within each beam (Sect. 2.2). However, this change would decrease the axial contribution (19)–(20), and the corresponding linearized bound would decrease. Then the medium would not be optimal anymore, according to the definition from Sect. 2.2.

It is useful to remark that directions of bars in optimal micro-trusses should be related to the principal directions of the applied macroload according to the theory of Michell trusses. This is directly related to the impossibility of full geometrical characterization of K^*- and G^*-optimal media. For $\mathbf{\Sigma}^K$ each direction is a principal direction. $\mathbf{\Sigma}^G$ can be determined by five non-zero and independent parameters, and therefore each direction can also be assumed as a principal one. Directions of bars are precisely specified in G_1^*- and G_2^*-optimal media. In the former case they coincide with the principal directions of the macroload, which are in this case unique for any $\mathbf{\Sigma}^{1G}$. However, in the latter case, the directions of bars could hardly be determined in such a way.

Other remarks emerge from comparison of the additional constraints (geometrical requirements) for K^*- and G^*-optimal media, (35) and (56), respectively. It can be shown, with the help of (26) and the second relation in (28), that the group of media satisfying (56) forms a subgroup of microstructures for which (35) holds. Therefore each K^*-optimal medium already fulfills additional constraints for G^*-optimal ones, consequently, it is hard to find a G^*-optimal medium that is not K^*-optimal.

It is straightforward to derive bounds for the Young's modulus for media with effective isotropy and cubic symmetry, respectively, in the form of

$$E^*_{is,+} = \frac{4K^*_+ G^*_+}{K^*_+ + G^*_+} = \frac{4\,(s/9)\,(s/15)}{(s/9)+(s/15)} = \frac{s}{6}\,,$$
$$E^*_{cs,+} = \frac{4K^*_+ G^*_{1,+}}{K^*_+ + G^*_{1,+}} = \frac{4\,(s/9)\,(s/6)}{(s/9)+(s/6)} = \frac{4}{15}s\,, \tag{58}$$

however, no conclusions can be taken on upper bounds on effective Poisson's ratios. It is only easy to verify that UPL have zero effective Poisson´s ratios. K^*- and at the same time G^*-optimal micro-trusses have an effective Poisson's ratio equal to 1/4, as shown by Bakhvalov and Panasenko (1989).

In the optimal micro-trusses it is interesting to see what the other elastic properties are. A summary is given in Table 7. Furthermore, in Table 8 bounds for open-cell foams proven in this article are compared with the composite ones. The composites bounds for effectively isotropic media are taken from Hashin and Shtrikman (1963) and Hashin (1970, 1983) and for media with effective cubic symmetry from Avellaneda (1987). They are specified for one void phase and linearized with respect to the material volume fraction. One can see that the solid-phase Poisson's ratio ν_s naturally appears in the linearized composite bounds (unlike the 2D case shown in Dimitrovová and Faria (1999)). This is because in optimal 3D media shell or plate parts must be

Table 7 Other elastic properties in optimal micro-trusses

Macro-load	Optimal micro-trusses	Other elastic properties K^*	G_1^*	G_2^*	G^*
$\mathbf{\Sigma}^K$	UPL, UDL, other media, which cannot be fully geometrically specified	K^*_+	not uniquely defined	not uniquely defined	not uniquely defined
$\mathbf{\Sigma}^{1G}$	only UPL	K^*_+	$G^*_{1,+}$	0	– –
$\mathbf{\Sigma}^{2G}$	only UDL	K^*_+	0	$G^*_{2,+}$	– –
$\mathbf{\Sigma}^G$	media that cannot be fully geometrically specified, but neither UPL nor UDL	not uniquely defined	G^*_+	G^*_+	G^*_+

Table 8 Composite bounds, bounds for open-cell foams and characterization of the optimal media

Composite bounds	$K_+^* = \frac{2s}{3\left(3\left(1-\nu_s\right)-s\left(1+\nu_s\right)\right)}$	$G_{1,+}^* = \frac{s\left(2-\nu_s\right)}{2\left(1+\nu_s\right)} \frac{1}{3\left(3\left(1-\nu_s\right)-s\left(1-2\nu_s\right)\right)}$	$G_{2,+}^* = \frac{s\left(5-3\nu_s\right)}{2\left(1+\nu_s\right)} \frac{1}{\left(9\left(1-\nu_s\right)-2s\left(2-3\nu_s\right)\right)}$	$G_+^* = \frac{s\left(7-5\nu_s\right)}{2\left(1+\nu_s\right)} \frac{1}{\left(15\left(1-\nu_s\right)-2s\left(4-5\nu_s\right)\right)}$
Linearized form	$\frac{2}{9\left(1-\nu_s\right)}s$	$\frac{2-\nu_s}{6\left(1-\nu_s^2\right)}s$	$\frac{5-3\nu_s}{18\left(1-\nu_s^2\right)}s$	$\frac{7-5\nu_s}{30\left(1-\nu_s^2\right)}s$
Previous form with $\nu_s = 0$	$\frac{2}{9}s$	$\frac{1}{3}s$	$\frac{5}{18}s$	$\frac{7}{30}s$
Bound for open-cell foams from this article	$\frac{1}{9}s$	$\frac{1}{6}s$	$\frac{1}{9}s+\beta s^2$	$\frac{1}{15}s+\eta s^2$
Optimal media are ...	determined by necessary and sufficient conditions	fully geometrically specified	fully geometrically specified	determined by necessary and sufficient conditions

included. β and η stand for coefficients of the bending contribution.

Finally, let us make some remarks about the simplified assumptions adopted for the strain energy contribution. It is known that assuming a micro-frame medium with theoretical lengths makes the medium softer than it really is. It is thus better to use beam active lengths and include the deformation of the joints. Moreover, the strain energy density corresponding to shear forces could be included in W. Obviously, such improvements do not change the linearized bounds since they do not influence expressions for the axial response of the media. If, e.g., the strain energy density corresponding to shear forces was included, the parameters β and η from Table 8 would decrease. In this case the solid-phase Poisson's ratio would appear in the final result.

Appendix

Admitting a more general solid material behavior it is possible to show that open-cell foam bounds coincide with the Voigt bound. For the sake of simplicity let us assume a 2D medium, the regular lattice, which is k^*- & G_1^*-optimal (Dimitrovová and Faria 1999). k^* stands for the 2D bulk modulus and G_1^* has the same meaning as before. The Voigt bounds k_V^* and $G_{1,V}^*$ for one void phase are (see Hill (1963)):

$$k_V^* = \frac{s}{2\left(1-\nu_s\right)}, \quad G_{1,V}^* = \frac{s}{2\left(1+\nu_s\right)},$$

where ν_s is the solid-phase Poisson's ratio. Now deformation of joints cannot be neglected, due to the presence of ν_s, which is restricted to the interval $[-1, 1]$. It is obvious that the strain field inside the cell of the regular lattice would be fully uniform for the $\mathbf{\Sigma}^k$ macroload only if $\nu_s = -1$, giving $k_V^* = s/4$, and for the $\mathbf{\Sigma}^{1G}$ macroload only if $\nu_s = 1$, yielding $G_{1,V}^* = s/4$, which are upper bounds on the moduli of 2D cellular media.

References

Allaire G, Aubry S (1999) On optimal microstructures for a plane shape optimization problem. Struct Optim 17:86–94

Allaire G, Kohn RV (1993) Optimal design for minimum weight and compliance in plane stress using extremal microstructures. Eur J Mech A/Solids 12:839–878

Avellaneda M (1987) Optimal bounds and microgeometries for elastic two-phase composites. J Appl Math SIAM 47:1216–1228

Bakhvalov N, Panasenko G (1989) Homogenization: averaging processes in periodic media. Kluwer Academic, Dordrecht

Bensoussan A, Lions JL, Papanicolau G (1978) Asymptotic analysis for periodic structures. North Holland, Amsterdam

Christensen RM (1994) Heterogeneous material mechanics at various scales. Appl Mech Rev 47:S20–S33

Christensen RM (1995) The hierarchy of microstructures for low density materials. Z angew Math Phys 46:S507–S521

Dimitrovová Z (1999) Effective constitutive properties of linear elastic cellular solids with randomly oriented cells. J Appl Mech ASME 66:918–915

Dimitrovová Z, Faria L (1999) New methodology to establish bounds on effective properties of cellular solids. J Mech Compos Mater Struct 6:331–346

Duvaut G (1976) Homogeneization et materiaux composite. In: Ciarlet P, Rouseau M (eds) Theoretical and applied mechanics. North Holland, Amsterdam

Gibson LJ, Ashby, MF (1988) Cellular solids. Structure and properties. Pergamon, Oxford

Gibianski LV, Sigmund O (2000) Multiphase elastic composites with extremal bulk modulus. J Mech Phys Solids 48:461–498

Grenestedt JL (1999) Effective elastic behavior of some models for 'perfect' cellular solids. Int J Solids Struct 36:1471–1501

Guedes JM, Rodrigues HC, Bendsoe MP (2003) A material optimization model to approximate energy bounds for cellular materials under multiload conditions. Struct Optim 25:446–452

Hashin Z (1962) The elastic moduli of heterogeneous materials. J Appl Mech ASME 29:143–150

Hashin Z (1970) Theory of composite materials. In: Wendt FW, Liebowitz H, Perrone N (eds) Mechanics of composite materials. Pergamon, Oxford

Hashin Z (1983) Analysis of composite materials - a survey. J Appl Mech ASME 50:481–505

Hashin Z, Shtrikman S (1962) A variational approach to the theory of the elastic behavior of polycrystals. J Mech Phys Solids 10:343–352

Hashin Z, Shtrikman S (1963) A variational approach to the theory of

the elastic behavior of multiphase materials. J Mech Phys Solids 11:127–140
Hill R (1963) Elastic properties of reinforced solids: some theoretical principles. J Mech Phys Solids 11:357–372
Kraynik AM, Warren WE (1994) The elastic behavior of low-density cellular plastics. In: Hilyard NC, Cunningham A (eds) Low density cellular plastics: physical basis of behavior. Chapman & Hall, London, pp217
Lekhnitskii SG (1981) Theory of elasticity of an anisotropic body. Mir, Moscow
Li K, Gao X-L, Roy AK (2003) Micromechanics model for three-dimensional open-cell foams using a tetrakaidecahedral unit cell and castigliano's second theorem. Compos Sci Tech 63:1769–1781
Nemat-Nasser S, Hori M (1993) Micromechanics: overall properties of heterogeneous materials. In: Achenbach J, Budiansky B, Lauwerier HA, Saffman PG, Van Wijngaarden L, Willis JR (eds) Series in applied mathematics and mechanics 37. North Holland, Amsterdam
Neves MM, Guedes JM, Rodrigues H (2000) Optimal design of periodic linear elastic microstructures. Comput Struct 76:421–429
Noor AK (1988) Continuum modeling for repetitive lattice structures. Appl Mech Rev 41:285–296
Sigmund O (1994) Materials with prescribed constitutive parameters: an inverse homogenization problem. Int J Solids Struct 31:2313–2329
Suquet PM (1985) Elements of homogenization for inelastic solid mechanics. In: Sanchez-Palencia E, Zaoui A (eds) Homogenization techniques for composite media, Lecture notes in physics 272. Springer, Berlin Heidelberg New York, pp193–278
Warren WE, Kraynik AM (1988) The linear elastic properties of open-cell foams. J Appl Mech ASME 55:341–346
Warren WE, Kraynik AM (1997) Linear elastic behavior of a low-density kelvin foam with open cells. J Appl Mech ASME 64:787–794
Zhu HX, Knott JF, Mills NJ (1997) Analysis of the elastic properties of open-cell foams with tetrakaidecahedral cells. J Mech Phys Solids 45:319–343